Analysis of tensile specific deformation of fiber reinforced concrete beams via FEM

Iva E. P. Lima[1], Aline S. R. Barboza[1]

[1]*Postgraduate Program in Civil Engineering, Federal University of Alagoas*
Av. Lourival Melo Mota, 57072-970, Maceio/Alagoas, Brazil
ivaemanuellyl@gmail.com, aline@lccv.ufal.br

Abstract. The use of fiber reinforced concrete (FRC) for structural purposes has been gradually increasing and this growth has resulted in the emergence of several standards. With regard to Brazil, the first standard related to FRC structures was published in 2021. In this standard, the calculation aspects for sizing FRC structures are represented, however, the behavior of tensile specific deformations is not fully illustrated. Based on this, a study is presented regarding the determination of the tensile specific deformation at the beginning of the plastic boundary (ε_{Fp}) of beams fiber reinforced concrete (FRC) and beams fiber reinforced high strength concrete (FRHSC). To establish these deformations, works found in the literature were used and the beams were analyzed using numerical analysis via the finite element method (FEM). According to the study carried out, it was found that, for FRC beams and FRHSC beams, ε_{Fp} corresponded to a value in the order of 5.0‰ and 6.5‰, respectively. This illustrates the possibility of greater deformation occurring at the beginning of the plastic boundary for the FRHSC and shows the potential of the work to contribute to the establishment of guidelines for the structural aspects of the FRC.

Keywords: fiber reinforced concrete, fiber reinforced high strength concrete, tensile specific deformation.

1 Introduction

The use of fiber reinforced concrete (FRC) for structural purposes has been gradually increasing on a global scale and has undergone several advances over the last 15 years. This evolution has been happening because research into fiber reinforced concrete began to highlight the application of fibers as a structural material, based on the development of fracture mechanics concepts to describe the residual tensile strength of the FRC due to the tensions transfer bridge mechanism [1], [2], [3].

Based on this, the development of fracture mechanics concepts must be based on the study of the residual resistance provided by fiber reinforcement, in which, based on constitutive laws, crack openings in the tensioned part of the concrete are observed. Thus, through the constitutive relationships for the design of fiber reinforced concrete structures, it is possible to develop the calculation aspects that must be considered to design a structural project produced with FRC elements [1], [4], [5].

Based on this, the use of the FRC for structural purposes has been consolidating over the last few years and this growth trend is exemplified by the emergence of several standards, such as the *fib* model code 2010 [6], the ACI 544.8R [7] and the NBR 16935 [8]. However, with regard to Brazil, although FRC has also been used in civil construction over the last 15 years, the first standardization related to the design of FRC structures was only published in 2021.

In this context, NBR 16935 [8] represents the calculation aspects that must be considered to design FRC structural elements, however, this same regulation does not fully illustrate the behavior of the tensile specific deformations of the FRC. Therefore, the need for more studies related to the design stage of fiber reinforced concrete structures is essential.

Based on this problem, this work presents a study regarding the determination of the tensile specific deformation at the beginning of the plastic boundary of beams fiber reinforced concrete (FRC) and beams fiber

reinforced high strength concrete (FRHSC), in which this parameter will allow a more complete analysis of the mechanical behavior of concrete.

2 Methodology

This chapter illustrates information regarding the configurations of the beams, the properties of the materials used and the data necessary for the numerical modeling of the beams are represented. It is worth mentioning that the information illustrated in this section refers to works found in the literature, but the calculated values (Tab. 2, 3, 4, 6, 7 and 8) and numerical modeling (section 3) were carried out by the authors of this work.

2.1 Beams fiber reinforced concrete – work of Freitas [9]

To carry out this study, beams with dimensions of 150 × 150 × 550 mm were produced with a test span of 500 mm, as recommended by EN 14651 [10] for the three-point bending test. Continuing, the beams were molded in two layers of the same dimensions, where the lower layer (from the base to half the height of the beam) was composed of steel fibers reinforced concrete (SFRC) and the upper layer (from half the height to the top of the beam) was formed from conventional concrete (CC). The characteristics of the materials used to make the beams are shown in Tab. 1.

Table 1. Characteristics of the materials used

Material	Aspect	Value
SFRC	Compressive medium strength (f_{cm})	36.89 MPa
	Poisson's coefficient (v)	0.2
	Longitudinal modulus of elasticity (E)	30.7 GPa
CC	Compressive medium strength (f_{cm})	33.95 MPa
	Poisson's coefficient (v)	0.2
	Longitudinal modulus of elasticity (E)	30.7 GPa
Steel fibers	Length (l_f)	60 mm
	Form factor (FF)	80
	Tensile strength (σ_y)	1100 MPa
	Fiber volume	0.16%

After applying the three-point bending test, results corresponding to the applied load, displacement and crack opening were obtained. From this, the stresses and strains in compression and tension were calculated, respectively (Tab. 2).

Table 2. Behavior in compression and tension, respectively – values calculated from the test

σ_c (MPa)	ε_c (m/m)	σ_c (MPa)	ε_c (m/m)	σ_t (MPa)	ε_t (m/m)	σ_t (MPa)	ε_t (m/m)
0.00	0.00000	12.44	0.00408	0.00	0.00000	0.62	0.02158
5.43	0.00224	12.86	0.00436	0.73	0.00436	0.58	0.02336
7.78	0.00285	12.05	0.01508	0.70	0.00593		
10.11	0.00344	9.82	0.02442	0.69	0.01508		
10.89	0.00364	8.79	0.02579	0.68	0.01754		
11.67	0.00385	8.10	0.02618	0.64	0.02029		

From the values shown in Tab. 1 and 2, we can begin determining the five CDP parameters, as can be seen in Tab. 3: expansion angle (ψ), ratio between the biaxial and uniaxial compression resistances (σ_{b0}/σ_{c0}), ratio between the traction and compression meridians in the diverter plane (K_c), flow potential eccentricity (e) and viscosity (μ). Note: For more details on establishing CDP parameters, see the work of Matos [11].

Table 3. Determination of the five CDP parameters

ψ	σ_{b0}/σ_{c0}	K_c	e	μ
32.17°	1.23	0.63	0.10	0.0001

Continuing with the determination of the parameters for modeling, the parameters that identify the

stress-strain relationship of the FRC were also established (Tab. 4). To establish these values, the results illustrated in Tab. 2 were used as an aid.

Table 4. Behavior in compression and tension, respectively – CDP parameters

σ_c (MPa)	ε^{in} (m/m)	σ_c (MPa)	ε^{in} (m/m)	σ_t (MPa)	ε^{ck} (m/m)	σ_t (MPa)	ε^{ck} (m/m)
0.00	0.0000	12.44	0.0037	0.00	0.0000	0.62	0.0216
5.43	0.0021	12.86	0.0039	0.73	0.0043		
7.78	0.0026	12.05	0.0147	0.70	0.0059		
10.11	0.0031	9.82	0.0241	0.69	0.0151		
10.89	0.0033	8.79	0.0255	0.68	0.0175		
11.67	0.0035	8.10	0.0259	0.64	0.0203		

Thus, with the illustration of these specifications, the numerical modeling of the beams molded by Freitas [9] can begin. It is worth mentioning that for the layer with SFRC, will be considered in elastic behavior and plastic behavior in the CDP, whereas for the CC layer, only elastic behavior will be considered.

2.2 Beams fiber reinforced high strength concrete – work of Mudadu *et al.* [12]

When preparing this study, beams were also produced as recommended by EN 14651 [10] for the three-point bending test. And in a similar way to that shown in section 2.1, the beams were also molded in two layers (lower layer composed of steel fibers reinforced high strength concrete – SFRHSC and upper layer composed of high strength concrete – HSC), as illustrated in Tab. 5.

Table 5. Characteristics of the materials used

Material	Aspect	Value
SFRHSC	Compressive medium strength (f_{cm})	56.4 MPa
	Poisson's coefficient (v)	0.2
	Longitudinal modulus of elasticity (E)	48.4 GPa
HSC	Compressive characteristic strength (f_{ck})	55 MPa
	Poisson's coefficient (v)	0.2
	Longitudinal modulus of elasticity (E)	48.4 GPa
Steel fibers	Length (l_f)	35 mm
	Form factor (FF)	64
	Tensile strength (σ_y)	1345 MPa
	Fiber volume	1.0%

After applying the three-point bending test, results corresponding to the applied stress and crack opening were obtained. From this, the tensions and deformations in compression and tension, respectively, were established (Tab. 6).

Table 6. Behavior in compression and tension, respectively – values calculated from the test

σ_c (MPa)	ε_c (m/m)	σ_c (MPa)	ε_c (m/m)	σ_t (MPa)	ε_t (m/m)	σ_t (MPa)	ε_t (m/m)
0.00	0.00000	50.49	0.01233	0.00	0.00000	6.01	0.02467
40.37	0.00094	49.21	0.01447	7.85	0.00667	5.85	0.02533
45.70	0.00133	47.93	0.01607	7.70	0.00800	5.61	0.02667
48.60	0.00200	46.71	0.01767	7.62	0.01033		
50.15	0.00267	44.01	0.02033	7.53	0.01167		
51.30	0.00333	41.72	0.02333	7.15	0.01533		
52.65	0.00580	40.97	0.02427	7.01	0.01700		
52.79	0.00620	39.96	0.02500	6.70	0.01900		
51.98	0.00833	38.48	0.02600	6.49	0.02113		
51.23	0.01100			6.14	0.02380		

In a similar way to what was shown in the previous section, based on the values shown in Tab. 5 and 6, we can begin determining the five CDP parameters (Tab. 7). And continuing, the parameters that identify the

stress-strain relationship of the FRC were also established for modeling in the CDP (Tab. 8).

Table 7. Determination of the five CDP parameters

ψ	σ_{b0}/σ_{c0}	K_c	e	μ
37.00°	1.57	0.67	0.10	0.0001

Table 8. Behavior in compression and tension, respectively – CDP parameters

σ_c (MPa)	ε^{in} (m/m)	σ_c (MPa)	ε^{in} (m/m)	σ_t (MPa)	ε^{ck} (m/m)	σ_t (MPa)	ε^{ck} (m/m)
0.00	0.0000	50.49	0.0113	0.00	0.0000	6.01	0.0245
40.37	0.0001	49.21	0.0134	7.85	0.0065	5.85	0.0252
45.70	0.0004	47.93	0.0151	7.70	0.0078	5.61	0.0266
48.60	0.0010	46.71	0.0167	7.62	0.0102		
50.15	0.0016	44.01	0.0194	7.53	0.0115		
51.30	0.0023	41.72	0.0225	7.15	0.0152		
52.65	0.0047	40.97	0.0234	7.01	0.0169		
52.79	0.0051	39.96	0.0242	6.70	0.0189		
51.98	0.0073	38.48	0.0252	6.49	0.0210		
51.23	0.0099			6.14	0.0237		

Thus, with the illustration of these specifications, the numerical modeling of the beams molded by Mudadu *et al.* [12] was started. It is important to mention that this modeling will occur in a similar way to the modeling in work Freitas [9].

3 Results and discussions

This chapter illustrates the steps carried out in modeling using the ABAQUS software, which are comprised of: creation of model parts, allocation of materials, idealization of the beam equivalent set, steps used, establishment of boundary conditions and loads, definition and convergence of the mesh, and determination of the tensile specific deformation at the beginning of the plastic boundary.

3.1 Beams fiber reinforced concrete – work of Freitas [9]

The first stage of modeling was to create the model, which took into account the dimensions and characteristics of the beam, as illustrated in EN 14651 [10]. Furthermore, the beam was molded in two layers of the same dimensions (bottom layer and top layer) and therefore a partition was made halfway up the height of the element. And in order to reproduce the equipment used, markings were made referring to the load application point and the machinery support supports, as illustrated in EN 14651 [10] (Fig. 1a).

After creating the model, the corresponding materials were assigned to each layer. For the layer with SFRC (lower layer), elastic behavior and plastic behavior in the CDP were considered (values shown in Tab. 1, 3 and 4), whereas for the CC layer (upper layer), only the was considered behavior elastic (values shown in Tab. 1). After that, the set equivalent to the analyzed beam was visualized (Fig. 1b).

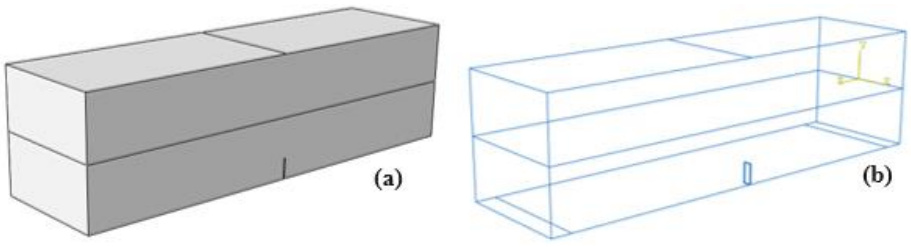

Figure 1. Modeling the work of Freitas [9]
(a) Model creation; (b) Ensemble view

Continuing, two steps were used: the first corresponds to static analysis referring to the supports and the second corresponds to static analysis with loading increments related to the application of the load. Afterwards, the boundary conditions relating to the machinery supports were established and the value corresponding to the load application was assigned. For the supports, in relation to the left side, translation restrictions were applied along the *x* and *y* axes, and in relation to the right side, translation restrictions were applied along the *x, y* and *z* axes. For loading, a translation of 3.38 mm was applied in the negative direction of the *y* axis and a translation constraint was applied along the *x* and *z* axes (Fig. 2a).

After applying the boundary conditions, the next step was to define the mesh. As an initial test to establish the mesh size, the fiber length was used as a parameter, so the first mesh analyzed was 60 mm long, and in relation to the shape of the mesh element, hexahedral elements were chosen. The Fig. 2b shows a mesh applied to the beams molded in Freitas [9].

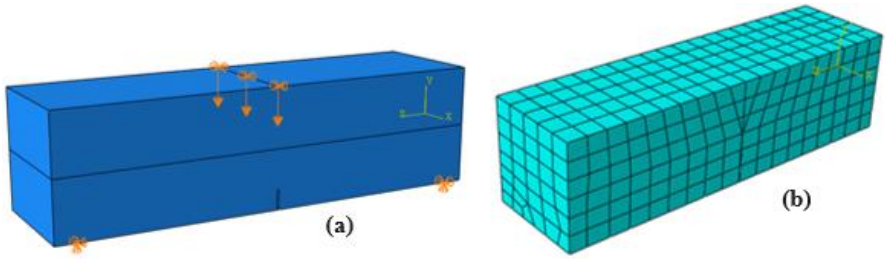

Figure 2. Modeling the work of Freitas [9]
(a) Application of boundary conditions; (b) Mesh representation

Based on the size of the first mesh, and to achieve the desired precision of the numerical results, other meshes with different sizes were analyzed and the mesh convergence study was carried out. For this, the maximum plastic deformation values of different refinement levels were evaluated (Tab. 9).

Table 9. Parameter analyzed in the study of meshes

Mesh	Time	Plastic deformation (m/m)	Variation (%)
60 mm	1 hour and 4 minutes	0.010277	-
50 mm	1 hour and 25 minutes	0.015510	+50.9
40 mm	3 hours and 10 minutes	0.016130	+4.0
30 mm	5 hours and 3 minutes	0.021740	+34.8

Observing Tab. 9, analyzing the smallest variations observed and taking into account the analysis processing time, the chosen mesh was 40 mm, since this mesh presents good precision and does not require excessive computational effort. Furthermore, it was decided to finalize the refinement study on the 30 mm mesh due to the analysis processing time and due to the variations observed in relation to the previous mesh. Thus, after establishing the mesh, the graph of stress *versus* strain of the 40 mm mesh was plotted to determine the tensile specific deformation at the beginning of the plastic boundary (Fig. 3).

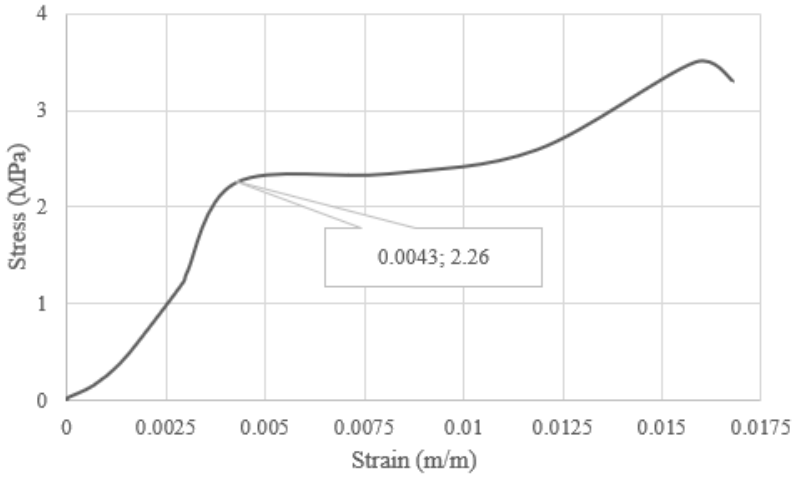

Figure 3. Stress *versus* strain

From Fig. 3, one can observe the behavior of stress versus strain equivalent to the modeling of the beam with a 40 mm mesh in the work of Freitas [9]. In analyzing Fig. 3, it can be seen that the deformation at the beginning of the plastic boundary occurs after deformation of the order of 4.3‰ and is equivalent to an approximate value of 5.0‰. Thus, analyzing the graph in a simplified way, it can be considered that the tensile specific deformation at the beginning of the plastic boundary for the FRC beams corresponds to a value in the order of 5.0‰.

3.2 Beams fiber reinforced high strength concrete – work of Mudadu *et al.* [12]

In a similar way to what was shown in the previous section, the first step was to create the model, where the dimensions and characteristics of the beam were taken into account, for example, the beam was molded in two layers of the same dimensions and a partition was made in the half the height of the element (Fig. 1a). After that, the corresponding materials were assigned to each layer. For the layer with SFRHSC (lower layer), elastic behavior and plastic behavior in the CDP were considered (values shown in Tab. 5, 7 and 8), whereas for the HSC layer (upper layer), it was considered only the behavior elastic (values shown in Tab. 5). After that, the set equivalent to the analyzed beam was visualized (Fig. 1b).

Continuing, two steps were used (static analysis and static analysis with loading increments). After that, the next step was to establish the boundary conditions. For the supports, in relation to the left side, translation restrictions were applied along the *x* and *y* axes, and in relation to the right side, translation restrictions were applied along the *x*, *y* and *z* axes. For the loading cleaver, a translation of 3.44 mm was applied in the negative direction of the *y* axis and a translation constraint was applied along the *x* and *z* axes, as can be seen analogously in the previous modeling (Fig. 2a). After this, the next step was to define the mesh and a length of 40 mm was used as an initial test to establish the mesh size. After that, the mesh convergence study was carried out (Tab. 10).

Table 10. Parameter analyzed in the study of meshes

Mesh	Time	Plastic deformation (m/m)	Variation (%)
40 mm	1 hour and 55 minutes	0.01064	-
35 mm	2 hours and 34 minutes	0.01146	+7.7
30 mm	5 hours and 40 minutes	0.01530	+33.5
29 mm	6 hours and 34 minutes	0.01570	+2.6

Observing Tab. 10, analyzing the smallest variations observed and taking into account the analysis processing time, the mesh chosen was 29 mm. Furthermore, taking into account the variations of the 29 mm mesh and the processing time of all meshes, it was preferred to finalize the mesh refinement study on the latter. Thus, after establishing the mesh for analysis, the graph of stress *versus* strain of the 29 mm mesh was plotted to determine the tensile specific deformation at the beginning of the plastic boundary (Fig. 4).

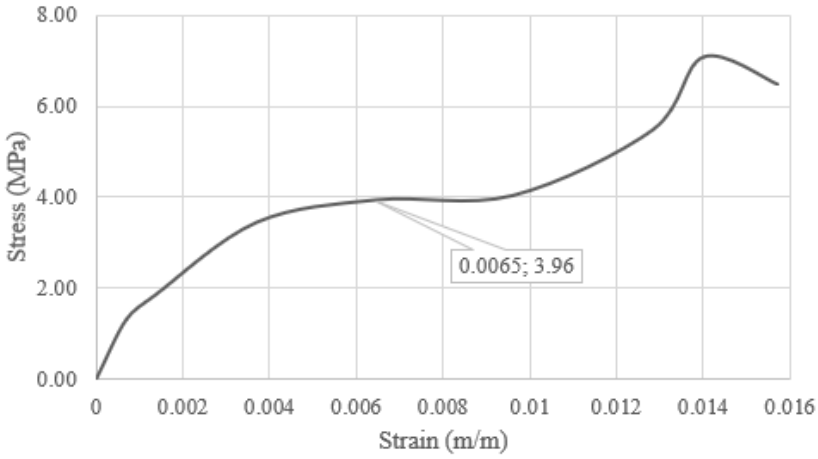

Figure 4. Stress *versus* strain

From Fig. 4, one can observe the behavior of stress versus strain equivalent to the modeling of the beam with a 29 mm mesh in the work of Mudado *et al.* [10]. In analyzing Fig. 4, it can be seen that the deformation at the beginning of the plastic boundary occurs slightly after deformation in the order of 6.5‰. Thus, analyzing the graph in a simplified way, it can be considered that the tensile specific deformation at the beginning of the plastic boundary for the FRHSC beams corresponds to a value in the order of 6.5‰. Therefore, and in accordance with

NBR 6118 [13], with Aslani *et al.* [14] and with Yang, Joh and Kim [15], it can be said that this behavior was already expected, since as the compression of the concrete increases, the tensile specific deformation can also increase at the beginning of the plastic boundary.

4 Conclusions

According to the investigation carried out, it was found that for FRC beams and FRHSC beams, the tensile specific deformation at the beginning of the plastic boundary corresponded to a value in the order of 5.0‰ and 6.5‰, respectively. This shows that as the compressive strength of the concrete increases, the deformation at the beginning of the plastic boundary is greater, and this happens because with the increase in the compressive strength of the material, the fragility of the concrete can also be increased, as for this type of composite, the cracks also develop through the aggregates, resulting in a relatively smoother fracture surface with less ductility.

From this, with the determination of these specific calculation deformations, it is possible to continue the study of the structural elements with the analysis of the deformation domains and consequently the adequate dimensioning of the structure, which shows the potential of the work in contributing to the establishment of guidelines for the structural aspects of fiber reinforced concrete. Therefore, it can be said that the present work achieved the initially suggested goals, where a study was presented regarding the determination of the tensile specific deformation at the beginning of the plastic boundary of FRC beams and FRHSC beams.

Authorship statement. The authors hereby confirm that they are the sole liable persons responsible for the authorship of this work, and that all material that has been herein included as part of the present paper is either the property (and authorship) of the authors, or has the permission of the owners to be included here.

References

[1] M. Di Prisco, M. Colombo and D. Dozio, "Fibre-reinforced concrete in *fib* Model Code 2010: Principles, models and test validation". *Structural Concrete***,** 2013.
[2] E. García-Taengua, M. Sonebi, P. Crossett, S. Taylor, P. Deegan, L. Ferrara and A. Pattarini, "Self-compactability and strength criteria for concrete mixes with mineral additions and fibres". *Concrete – Innovation and Design, fib Symposium*, Copenhagen May 18-20, 2015.
[3] L. Martinie and N. Roussel, "Simple tools for fiber orientation prediction in industrial practice". *Cement and Concrete Research*, 2011.
[4] P. Martinelli, M. Colombo, P. Pujadas, A. De La Fuente, S. Cavalaro and M. Di Prisco, "Characterization tests for predicting the mechanical performance of SFRC floors: identification of fibre distribution and orientation effects". *Materials and Structures*, 54:1, 2021a.
[5] P. Martinelli, M. Colombo, P. Pujadas, A. De La Fuente, S. Cavalaro and M. Di Prisco, "Characterization tests for predicting the mechanical performance of SFRC floors: design considerations". *Materials and Structures*, 54:2, 2021b.
[6] Fédération Internationale du Béton – FIB. "*fib* model code for concrete structures 2010". Switzerland, 2013.
[7] American Concrete Institute. "ACI 544.8R-16**"**: Indirect method for obtaining the stress/strain response of fiber-reinforced concrete (FRC). Dubai, 2016.
[8] Brazilian Association of Technical Standards. "ABNT NBR 16935": Design of fiber reinforced concrete structures – Procedure. Rio de Janeiro, 2021.
[9] D. J. P. Freitas, "Structural behavior of fiber reinforced concrete elements molded in layers". Federal University of Alagoas. Maceio, 2020.
[10] European Committee for Standardization. "EN 14651": Test method for metallic fiber-reinforced concrete – Measuring the flexural tensile strength (limit of proportionality (LOP), residual), CEN, London. 2007.
[11] C. C. D. Matos, "Numerical analysis of concrete beams reinforced with steel fibers using the finite element method". Postgraduate Program in Civil Engineering: Federal University of Rio Grande do Sul. Porto Alegre, 2021.
[12] A. Mudadu, G. Tiberti, F. Germano, G. Plizzari and A. Morbi, "The effect of fiber orientation on the post-cracking behavior of steel fiber reinforced concrete under bending and uniaxial tensile tests". *Cement and Concrete Composites*, 2018.
[13] Brazilian Association of Technical Standards**.** "ABNT NBR 6118": Design of reinforced concrete structures – Procedure. Rio de Janeiro, 2023.
[14] F. Aslani, F. Hamidi, A. Valizadeh and A. T. N. Dang, "High-performance fibre-reinforced heavyweight self-compacting concrete: analysis of fresh and mechanical properties". *Construction and Building Materials*, n. 232, 2020.
[15] I. H. Yang, C. Joh and B. S. Kim, "Structural behavior of ultra high performance concrete beams subjected to bending". *Engineering Structures*, n. 32, pp. 3478–3487, 2010.